ARTICLE IN PRESS
STOTEN-20306; No of Pages 14

Science of the Total Environment xxx (2016) xxx–xxx

Contents lists available at ScienceDirect

Science of the Total Environment

journal homepage: www.elsevier.com/locate/scitotenv

Application of Dempster–Shafer theory, spatial analysis and remote sensing for groundwater potentiality and nitrate pollution analysis in the semi-arid region of Khuzestan, Iran

Omid Rahmati [a,*], Assefa M. Melesse [b]

[a] Department of Watershed Management Engineering, College of Agriculture, Lorestan University, Lorestan, Iran
[b] Department of Earth and Environment, AHC-5-390, Florida International University, USA

HIGHLIGHTS

- Suitability map for drinking water was assessed using new methodological framework.
- The study applied DS theory of evidence for groundwater quantity analysis.
- Results of applied models were combined and its efficiency was assessed.
- The groundwater quality–quantity map showed 87.76% accuracy.
- The 'non acceptable' areas covers the highest part of the study area with 60%.

GRAPHICAL ABSTRACT

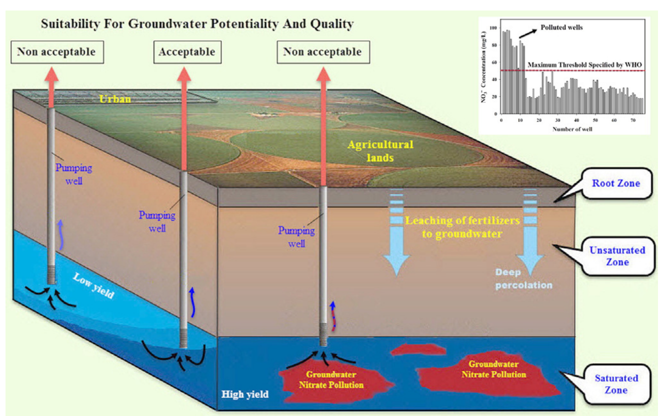

ARTICLE INFO

Article history:
Received 1 April 2016
Received in revised form 20 June 2016
Accepted 21 June 2016
Available online xxxx

Editor: D. Barcelo

Keywords:
Groundwater management
Environmental policies
Contamination
GIS
Remote sensing
Iran

ABSTRACT

Effective management and sustainable development of groundwater resources of arid and semi-arid environments require monitoring of groundwater quality and quantity. The aim of this paper is to develop a reasonable methodological framework for producing the suitability map for drinking water through the geographic information system, remote sensing and field surveys of the Andimeshk-Dezful, Khozestan province, Iran as a semi-arid region. This study investigated the delineation of groundwater potential zone based on Dempster–Shafer (DS) theory of evidence and evaluate its applicability for groundwater potentiality mapping. The study also analyzed the spatial distribution of groundwater nitrate concentration; and produced the suitability map for drinking water. The study has been carried out with the following steps: i) creation of maps of groundwater conditioning factors; ii) assessment of groundwater occurrence characteristics; iii) creation of groundwater potentiality map (GPM) and model validation; iv) collection and chemical analysis of water samples; v) assessment of groundwater nitrate pollution; and vi) creation of groundwater potentiality and quality map. The performance of the DS was also evaluated using the receiver operating characteristic (ROC) curve method and pumping test data to ensure its generalization ability, which eventually, the GPM showed 87.76% accuracy. The detailed analysis of groundwater potentiality and quality revealed that the 'non acceptable' areas covers an area of about

* Corresponding author.
E-mail addresses: omid_rahmati@ut.ac.ir, orahmati68@gmail.com (O. Rahmati), melessea@fiu.edu (A.M. Melesse).

http://dx.doi.org/10.1016/j.scitotenv.2016.06.176

Please cite this article as: Rahmati, O., Melesse, A.M., Application of Dempster–Shafer theory, spatial analysis and remote sensing for groundwater potentiality and nitrate pollution an..., Sci Total Environ (2016), http://dx.doi.org/10.1016/j.scitotenv.2016.06.176

1479 km^2 (60%). The study will provide significant information for groundwater management and exploitation in areas where groundwater is a major source of water and its exploration is critical to support drinking water need.

1. Introduction

The regular monitoring and management of groundwater potentiality and quality are very important for the sustainable development in arid and semi-arid regions. Access to drinking water in arid environments is an endemic challenge, especially in developing countries (Chen and Xue, 2003; Elmahdy and Mohamed, 2015; Sternberg and Paillou, 2015). Lack of safe fresh water supply is a recognized problem in Iran, where the expansion of irrigation activities, industrialization and urbanization are almost dependent on groundwater (Rahmati et al., 2014, 2016). In addition, groundwater nitrate pollution is the water quality issue of primary concern affecting the majority of aquifers in Iran, mostly due to anthropogenic activities including intense agriculture and urbanization (Jalali, 2011; Neshat and Pradhan, 2015; Rahmati et al., 2015; Masoud et al., 2016). From the health risk viewpoint, nitrate pollution of groundwater has adverse effects on human health, mainly causing methemoglobinemia in infants but also in the elderly and pregnant women (Sajil et al., 2014) and hence, nitrate concentration should be limited to below 50 (mg/L), World Health Organization's acceptable threshold in drinking water. In addition, Suthar et al. (2009) stated that the consumption of water contaminated with nitrate may cause multiple sclerosis, gastric cancer, thyroid gland hypertrophy, and Non-Hodgkin lymphoma among other health conditions. According to previous studies (McLay et al., 2001; Pathak and Hiratsuka, 2011; Kurunc et al., 2016), although aquifers are often the principal water supply in arid regions, groundwater resources are vulnerable to contamination due to inherent geological properties of aquifers (i.e. aquifer's vulnerability to leaching) and anthropogenic activities such as intense agriculture and urbanization. Therefore, simultaneous assessment and monitoring of the groundwater potentiality and quality is important for sustainable use of this valuable natural resource (Elewa and Qaddah, 2011; Oikonomidis et al., 2015). However, the main aim of sustainable groundwater management is to present different transferable methodologies that can be used globally due to lack of sufficiently detailed information regarding the hydrology, hydro-geology, and environments in some countries.

The term “groundwater potentiality” can be defined as possibility of groundwater occurrence or the amount of groundwater available in an area and it is a function of several geo-environmental conditioning factors (Jha et al., 2010). The traditional approaches of groundwater exploration are drilling, hydrogeological, geological and geophysical methods. These techniques have a good accuracy in assessing the groundwater potentiality, but are costly and time-consuming (Todd and Mays, 1980; Jha et al., 2010; Elmahdy and Mohamed, 2014). So, the development of reliable analytical methods for spatial prediction of groundwater potentiality and quality is urgently needed for efficient management and sustainable use of groundwater resources.

In recent years, many methodologies have been applied by several researchers to produce the groundwater potentiality map (GPM). In some studies, data mining models such as frequency ratio (FR) (Oh et al., 2011; Davoodi Moghaddam et al., 2015), weights-of-evidence (WOE) (Ozdemir, 2011; Lee et al., 2012a; Pourtaghi and Pourghasemi, 2014), evidential belief function (EBF) (Nampak et al., 2014; Pourghasemi and Beheshtirad, 2014; Tahmassebipoor et al., 2015; Ghorbani Nejad et al., 2016), and certainty factor (CF) (Razandi et al., 2015) have been used for assessing groundwater potentiality. Furthermore, numerous studies have described the application of the logistic regression (LR) (Ozdemir, 2011; Pourtaghi and Pourghasemi, 2014), artificial neural network model (ANN) (Lee et al., 2012b), random forest (Rahmati et al., 2016), and analytical hierarchy process (AHP) (Adiat et al., 2012; Rahmati et al., 2014; Shekhar and Pandey, 2014) for preparing the GPM. Elewa and Qaddah (2011) applied a geographic information system (GIS)-watershed-based modeling to identify the groundwater potential areas in the Sinai Peninsula, Egypt. They used eight conditioning factors including rainfall, lithology or infiltration, net groundwater recharge, lineament density, drainage density, slope, depth to groundwater, and water quality. Oikonomidis et al. (2015) proposed a GIS-based AHP methodology for assessing the groundwater potentiality and quality in Tirnavos area, Greece.

Most of past studies have focused on the GIS-based models to produce the GPM (Mills and Shata, 2009; Manap et al., 2013; Tahmassebipoor et al., 2015). Furthermore, the prior mentioned probability methods and the simple data mining techniques are capable of only handling stochastic uncertainty, hence, the systemic uncertainty is ignored. However, there are very few comprehensive studies about integrated assessment of groundwater potentiality and quality. Also, the method should consider both stochastic and systemic uncertainty in spatial prediction of groundwater and data integration. Therefore, from integrated groundwater resources management viewpoint, there is significant demand for simultaneously evaluating groundwater potentiality as well as its quality with high predictive accuracy.

This study is an attempt to investigate and understand groundwater potentiality of Andimeshk-Dezful region, Khozestan province, Iran using both groundwater quality and quantity aspects, by an integrated approach of remote sensing (RS), GIS, field work and lab techniques. The specific objectives of this study were to (i) delineate the groundwater potential zone via Dempster–Shafer (DS) theory of evidence and evaluate its applicability for groundwater potentiality mapping; (ii) determine the spatial distribution of groundwater nitrate concentration; and (iii) integrate groundwater potentiality and quality and producing suitability map for drinking water. The simultaneous application of DS model and nitrate concentration analysis in groundwater potentiality mapping provides originality to this study.

2. Study area

Andimeshk-Dezful region is a part of Khozestan province, Iran (Fig. 1). It is located between 31° 58′ and 32° 33′ N latitude, and 48° 01′ and 48° 46′ E longitude. The region is located in arid region and characterized with an average annual precipitation of 341 mm. The average daily minimum and maximum temperatures are 7.5 °C in the winter and 46 °C in the summer, respectively. The region occupies an area of 2464.75 km^2 with a population of 385,000. About 85% of Andimeshk-Dezful's irrigation and drinking water requirements are met through groundwater extraction. It consists of two major drainage networks emerging dominantly from the adjoining northern mountain ranges. The intensive farming activities and continuous extraction of groundwater have led to dramatic depleting in groundwater quality and quantity (Chandrakanth, 2015; Xue et al., 2015). This shows the need to develop a methodological framework for producing the suitability map for drinking water. Geologically, the region is located within the Zagros Structural Zone and consists of highly fractured Quaternary units (Alavi, 1994; Heyvaert and Baeteman, 2007).

3. Materials and methods

The methodological approach (Fig. 2) can be summarized in the following points:

i. creation of maps of groundwater conditioning factors;
ii. assessment of groundwater occurrence characteristics;
iii. creation of groundwater potentiality map and model validation;

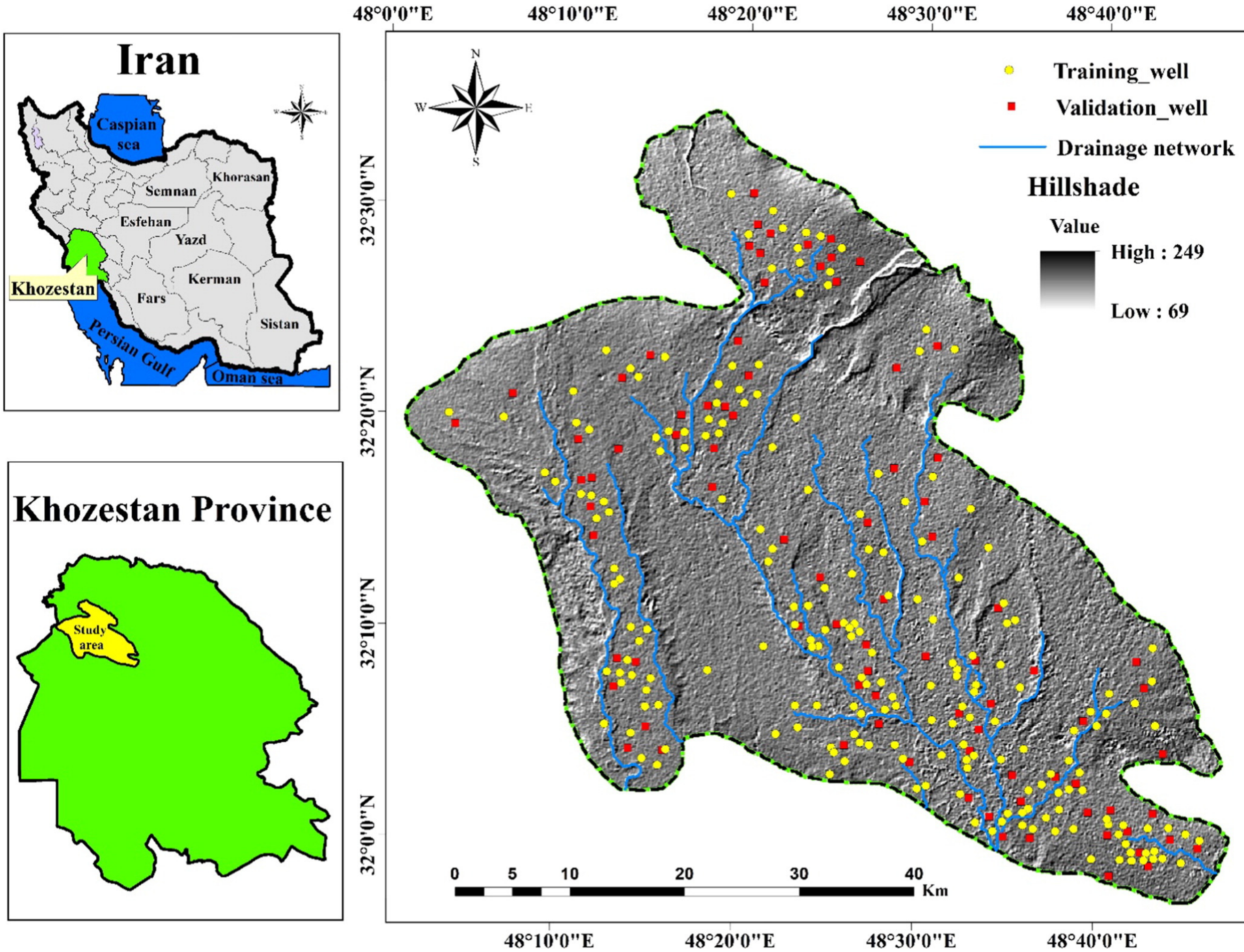

Fig. 1. Groundwater well locations map with a hill-shaded map of Dezful-Andimeshk region, Khozestan, Iran.

iv. collection and chemical analysis of water samples;
v. assessment of groundwater nitrate pollution; and
vi. creation of groundwater potentiality and quality map.

These steps are described in more detail in the next subsections.

3.1. Construction of groundwater conditioning factors

In this study, a total of nine conditioning factors were used through the knowledge attained from the literature, including lithology, land use, soil, altitude, slope percent, distance from river, river density, topographic wetness index (TWI), and lineament density (Adiat et al., 2012; Lee et al., 2012a,b; Elmahdy and Mohamed, 2014; Park et al., 2014; Razandi et al., 2015). Generally, the occurrence and potentiality of groundwater in a given area is governed by several conditioning factors. These factors are geological structure, lithology, fracture density, aperture and connectivity of fractures, secondary porosity, topography, landform, land use and land cover, groundwater recharge, groundwater table distribution, drainage pattern, and climatic condition (Oh et al., 2011; Ozdemir, 2011). No exact agreement exists on which factors should be used in groundwater potentiality analysis. However, some of the geo-environmental variables are mostly applied by several researchers which reflect their importance and role in groundwater studies (Elewa and Qaddah, 2011; Manap et al., 2013). To assess groundwater potentiality, the spatial geodatabase was considered to be a set of related conditioning factors that influence on groundwater occurrence and distribution. In the groundwater potentiality modeling, all conditioning factor layers were entered into a GIS environment and converted from vector to raster formats. A brief description of each conditioning factor is given below.

3.1.1. Lithology

Lithology has a key role in determining the groundwater potentiality due to the nature of the geological formations and its interaction on infiltration rates. Hence, it is considered as an important factor in previous studies (Pradhan, 2009; Adiat et al., 2012). The lithology map was extracted from the geologic thematic layer at the scale of 1:100,000, which was obtained from the Iranian Department of Geology Survey (IDGS) (Fig. 3a). According to this figure, the lithology of the study area is varied, and covered by conglomerate locally with sandstone (Plbk), and low level piedmont fan and valley terrace deposits (Q_{ft2}). Brief lithological details are given in Table 1.

3.1.2. Land use

In this study, the Landsat 7 Enhanced Thematic Mapper plus (ETM^+) images downloaded from the US Geological Survey (USGS) (http://earthexplorer.usgs.gov/) were used to produce land use map of the study area based on false color composite and pixel based supervised image classification techniques (Lillesand et al., 2008). After image classification, accuracy assessment was performed using data from field surveys and ground truth which were not utilized in the classification

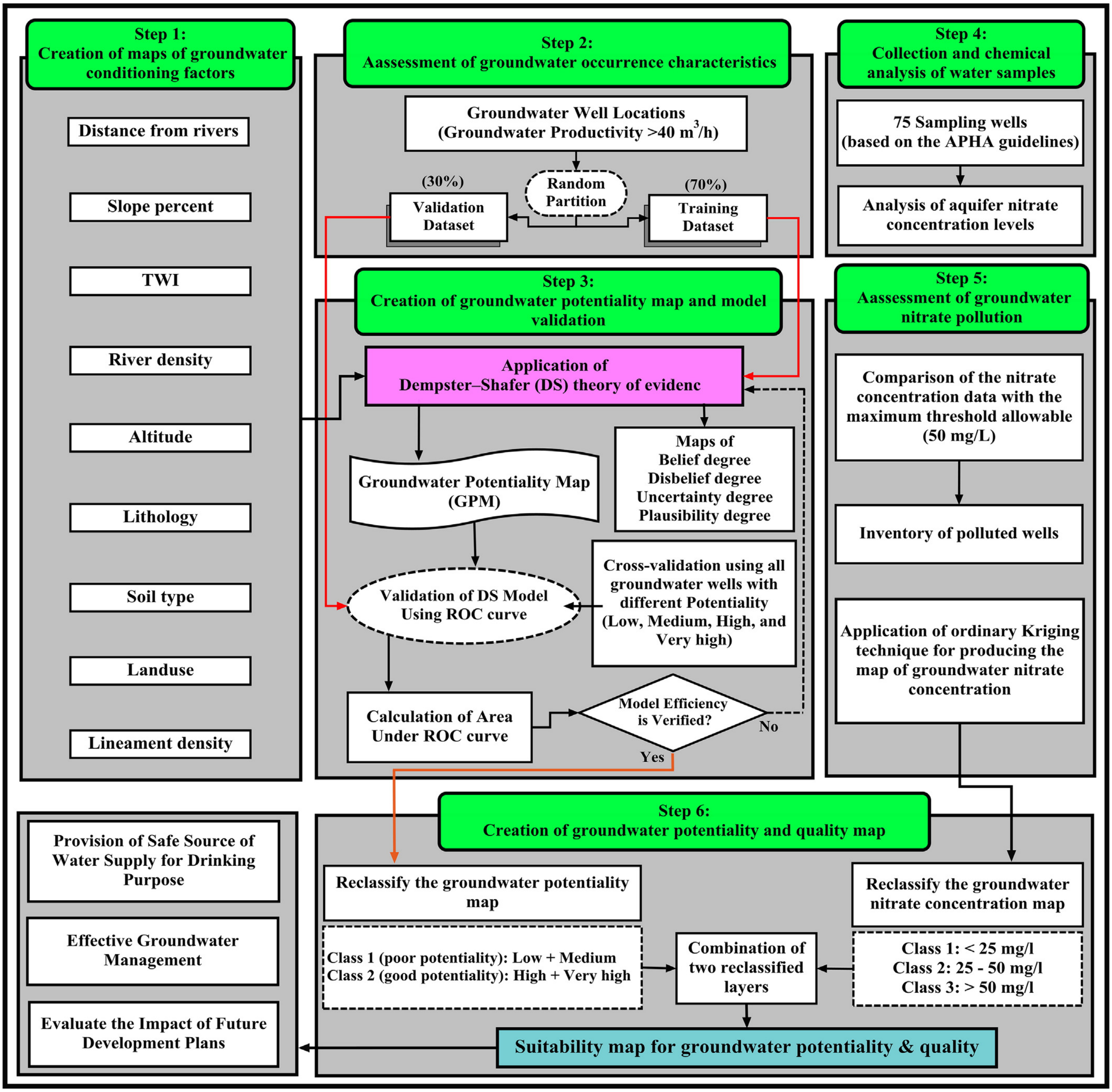

Fig. 2. Methodological flowchart of the study.

stage. Seven land use types, including bare land, dry farming, range land, river and riparian zones, urban area, wetland, and irrigated agriculture were classified (Fig. 3b).

3.1.3. Soil

The water infiltration depends on soil properties, and affects the subsurface flow and groundwater recharge; therefore, soil factor was included in the analysis. The 1:50,000 soil map was digitized from exploratory soil map of Khozestan province which was obtained from the Iranian Water Resources Department (IWRD). Then, the soil map was extracted as polygon features and converted to grid. The most dominant soil types of the study area are badland soil, Entisols and Inceptisols (Fig. 3c).

3.1.4. Altitude

As a first step, a digital elevation model (DEM) (with 20 × 20 m grid size) was generated from the topographic map of 1:25,000 scale provided by the Agency of Geographical Survey, Iran. The original altitude values vary between 38 and 244 m, and the values were reclassified into five classes with an interval of 50 m (Fig. 3d).

3.1.5. Slope

Another factor related to the runoff generation, and groundwater recharge and potentiality is slope percent (Adiat et al., 2012). The DEM was used to create the slope map. In the study area, the slope percent ranges between 0 and 24%. The slope percent values were divided into five categories (Fig. 3e) which are most widely used subdivisions in Iran (Rahmati et al., 2014).

Please cite this article as: Rahmati, O., Melesse, A.M., Application of Dempster–Shafer theory, spatial analysis and remote sensing for groundwater potentiality and nitrate pollution an..., Sci Total Environ (2016), http://dx.doi.org/10.1016/j.scitotenv.2016.06.176

3.1.6. Distance from river and river density

The stream network of the study area is extracted from the DEM layer and existing sources using the ArcHydro tools in ArcGIS, a spatial analysis software. From the stream network layer, distance from river and river density maps were produced by Euclidean distance and line density tools, respectively. In this study, distance from river is divided into 5 classes (Fig. 3f) and river density layer is reclassified into four classes: <0.1, 0.1–0.2, 0.2–0.3, and >0.3 km/km^2 (Fig. 3g).

3.1.7. Topographic wetness index (TWI)

Several researchers have used TWI for groundwater potentiality assessment (Pourghasemi and Beheshtirad, 2014; Pourtaghi and Pourghasemi, 2014; Falah et al., 2016). According to Rodhe and Seibert (1999) and Davoodi Moghaddam et al. (2015), the topography has a decisive role in the spatial variation of hydrological conditions (e.g. soil moisture) and determining the groundwater flow pattern. The TWI, as a secondary topographic factor, interprets the relation between the water inclination that accumulates at any point of the area and the gravitational force to move that water down slope. Water related factor of TWI was calculated using the following equation (Moore et al., 1991):

$$\mathrm{TWI} = \ln\left(\frac{A_s}{\tan\beta}\right) \tag{1}$$

where A_s and $\tan\beta$ are the specific catchment area and the slope angle at the point, respectively. In this study, TWI was reclassified into four classes (Fig. 3h).

3.1.8. Lineament density

Lineaments are linear features of tectonic origin which is related to hydrogeological conditions resulting in increased secondary porosity and permeability (Travaglia and Dianelli, 2003; Adiat et al., 2012). In this study, image enhancement (edge enhancement), Sobel directional filtering, and high-pass directional filtering (Saraf and Choudhury, 1998; Tam et al., 2004) were done on the Landsat ETM$^+$ image to

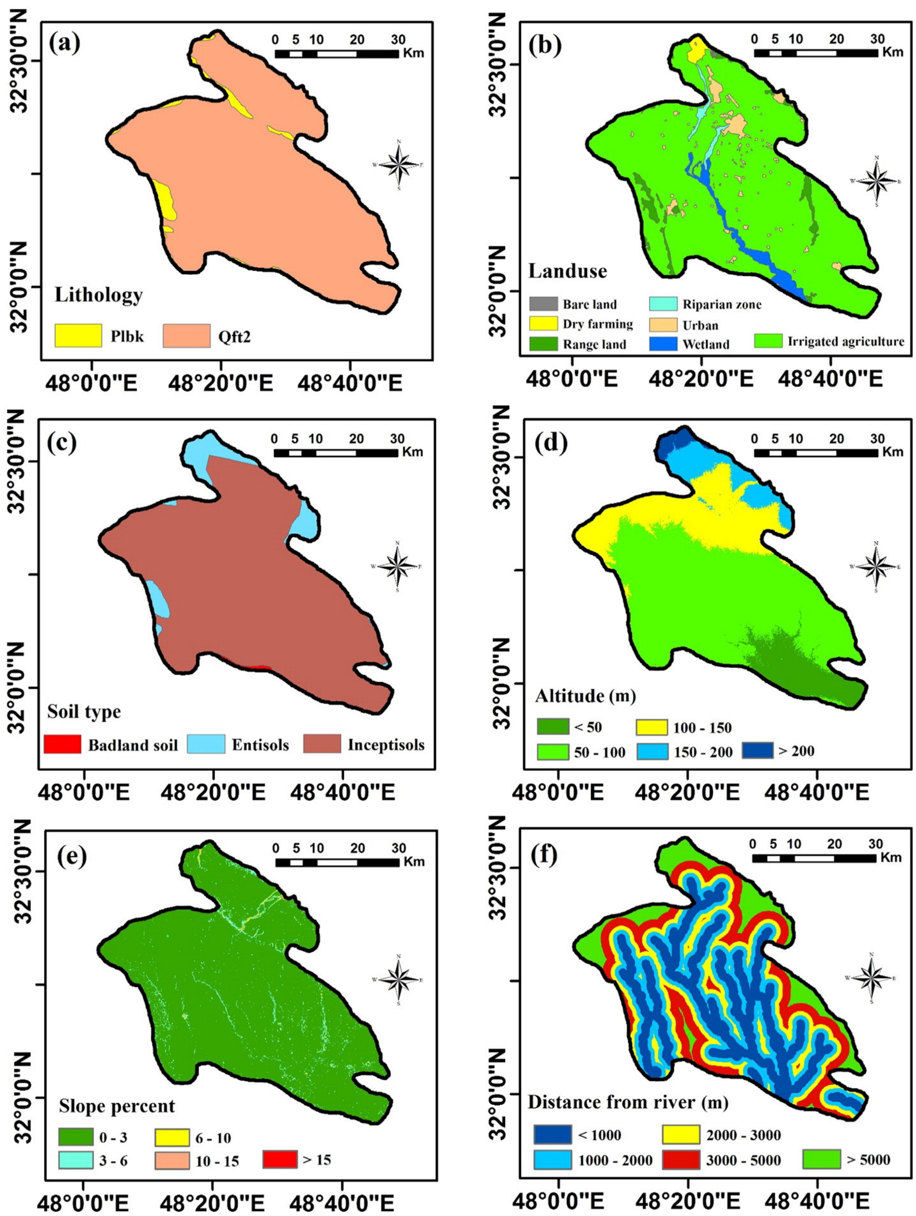

Fig. 3. Groundwater conditioning factors; (a) lithology, (b) land use, (c) soil type, (d) altitude, (e) slope percent, (f) distance from river, (g) river density, (h) TWI, and (i) lineament density.

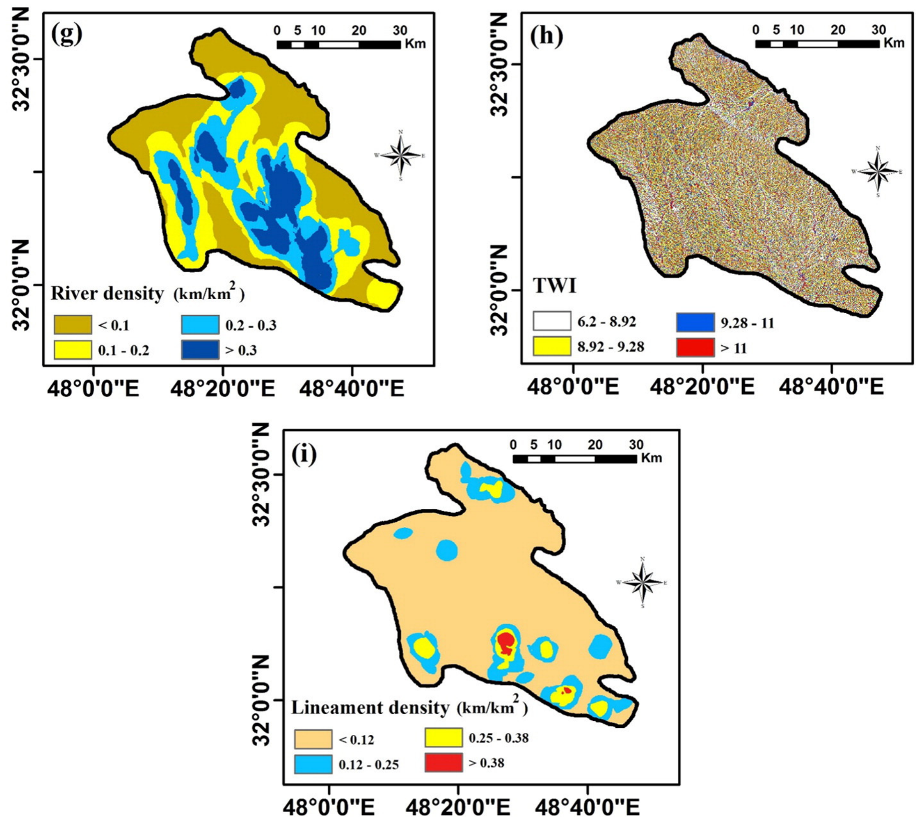

Fig. 3 (*continued*).

extract lineament and generate lineaments map of the area. Then, the lineament density map was produced using the line density tool in ArcGIS. The lineament density map was constructed with four categories as <0.12, 0.12–0.25, 0.25–0.38, and >0.38 km/km^2 (Fig. 3i).

Finally, all the layers were converted to a raster grid with 20 × 20 m cells—rasterized at a 20 m resolution—for application in groundwater potentiality modeling.

3.2. Assessment of groundwater occurrence characteristics

In this study, groundwater productivity data (i.e. groundwater yield) as derived from actual pumping tests, were obtained from Iranian Department of Water Resources Management (IDWRM). In the year 2010, IDWRM did set up standard of groundwater potential classification, which is based on yield value of well production. Following Razandi et al. (2015), the groundwater yield value >40 m^3/h was determined as high productivity value. In total, 288 groundwater wells with high potential yield values of ≥40 m^3/h were selected and imported in a GIS environment. Out of 288, 202 (70%) groundwater wells were randomly selected for model training (Fig. 1).

3.3. Application of DS model

In this study, Dempster–Shafer (DS) model was used to produce the groundwater potentiality map. The DS theory of evidence was originally introduced by Dempster (1967), considered as a spatial integration model with mathematical representation, and was later expanded upon by Shafer (1976). The theory and the algorithm of DS model, as well as its application in groundwater potentiality assessment, have been presented in Mogaji et al. (2014) and Nampak et al. (2014). In groundwater potentiality analysis based on the DS model, a structure of discernment can be considered as follows (Dempster, 1967; Shafer, 1976):

$$m: 2^{\Theta} = \{\phi, T_p, \overline{T}_p, \Theta\} \ \ with\ \Theta = \{T_p, \overline{T}_p\} \tag{2}$$

where T_P indicates a goal: "at each pixel p, it will be influenced by future groundwater occurrences". The function m:2^{Θ}→[0,1] is called a basic probability assignment when

$$\mathrm{m}(\varnothing) = 0 \tag{3}$$

and

$$\sum_{A \subset \Theta} \mathrm{m}(\mathrm{L}) = 1 \tag{4}$$

where L is a subset of Θ. The function m is considered as a measure of belief committed to each possibility (Walley, 1987). Based on mass function, belief (B) function can be defined by Eqs. (5), (6), (7), and (8). B committed to a proposition M is given by

$$\mathrm{B(M)} = \sum_{\mathrm{A \subset M}} f(\mathrm{L}) = 1 \tag{5}$$

The function m:2^{Θ} → [0,1] is called the belief function over frame Θ, if and only if it satisfies the following conditions:

$$\mathrm{B}(\varnothing) = 0, \tag{6}$$

Table 1
Lithology of the Dezful-Andimeshk region, Khozestan, Iran.

Code	Lithology	Formation	Geological age
Plbk	Conglomerate locally with sandstone	Bakhtyari	Pliocene
Q_{ft2}	Low level piedmont fan and valley terrace deposits	–	Quaternary

Please cite this article as: Rahmati, O., Melesse, A.M., Application of Dempster–Shafer theory, spatial analysis and remote sensing for groundwater potentiality and nitrate pollution an..., Sci Total Environ (2016), http://dx.doi.org/10.1016/j.scitotenv.2016.06.176

$$B(\Theta) = 1, \tag{7}$$

and for every collection of possibilities $L_1, L_2, \ldots, L_n$ of a subset of Θ and every positive integer n

$$B(L_1 \cup \ldots \cup L_n) \geq \sum_{\substack{I \subset \{1 \ldots n\} \\ I \neq \phi}} * (-1)^{|I|+1} B(\cap_{i \in I} L_i) \tag{8}$$

The plausibility (P) function $P{:}2^{\Theta} \rightarrow [0,1]$ is defined by using the belief (B) function as

$$P(M) = 1 - B(\overline{M}) = \sum\nolimits_{A \subset \Theta} f(L) - \sum\nolimits_{A \subset M} f(L) = \sum\nolimits_{L \cap M \neq \varnothing} m(L) \tag{9}$$

for every $M \subset \Theta$, where $\overline{M}$ is the negation of M.

The B and P functions are the lower and upper envelopes of a class of probability assignments about M so that $B_{(M)} \leq P_{(M)}$.

Park (2010) gives predictive groundwater potentiality mapping zones and also the degree of uncertainty of the same zone. The DS model provides framework for estimation of evidential belief functions (EBFs). The EBFs are compound of degrees of belief (B), disbelief (D), uncertainty (U), and plausibility (P), each in the range [0, 1] (Carranza et al., 2005). The schematic representation of this combination is shown in Fig. 4. Once the evidential belief functions are computed for all the groundwater conditioning factors, the Dempster–Shafer's rule of combination was applied to estimate the degrees of belief (B), disbelief (D), uncertainty (U), and plausibility (P) as follows:

$$B = \frac{\lambda(T_p E_{ij})}{\sum \lambda(T_p) E_{ij}} \tag{10}$$

$$D = \frac{\lambda(T_{\bar{p}}) E_{ij}}{\sum \lambda(T_{\bar{p}}) E_{ij}} \tag{11}$$

$\lambda(T_p)E_{ij}$ and $\lambda(T_{\bar{p}})E_{ij}$ were calculated using Eqs. (12) and (13), respectively.

$$\lambda(T_p)E_{ij} = \frac{[N(W \cap E_{ij})/N(W)]}{[(N(E_{ij}) - N(W \cap E_{ij}))/(N_A - N_W)]} \tag{12}$$

$$\lambda(T_{\bar{p}})E_{ij} = \frac{[N(W) - N(W \cap E_{ij})] \big/ N(W)}{[N(A) - N(W) - N(E_{ij})] \big/ [N(A) - N(W)]} \tag{13}$$

where $N(W \cap E_{ij})$, N(W), and N(A) are number of groundwater well pixels in the domain, total number of groundwater wells, and total number of pixels in the domain, respectively. The uncertainty (U), and plausibility (P) values were calculated using Eqs. (14) and (15).

$$U = 1 - D - B \tag{14}$$

$$P = 1 - D \tag{15}$$

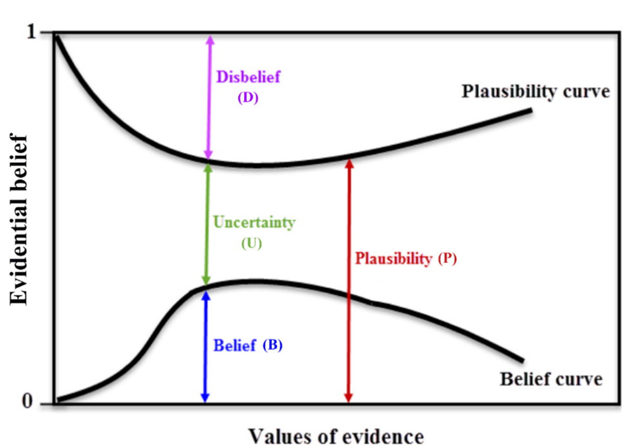

Fig. 4. Schematic relationships of evidential belief functions.

A detail description of the mathematical formulation of DS model can be found in Kim and Swain (1989).

In order to apply the DS model, first, the thematic layers (i.e. groundwater conditioning factors) should be transformed into evidential data layers that can be integrated to generate a predictive GPM by exploiting the quantitative knowledge of the spatial relationship between well locations and the groundwater conditioning factors (Neshat and Pradhan, 2015). DS model can be used to define the mass functions employing quantitative relationships between the known groundwater well locations (with high productivity) and input conditioning factors. In this context, groundwater productivity data (i.e. training dataset) were set as dependent variables, and several geo-environmental factors, which are known to influence groundwater productivity/potentiality, were considered as independent variables. Thus, after calculation of the weight values for each conditioning factor, groundwater potentiality map (GPM) was prepared by integration of factors' weight value, which were obtained from Belief values.

3.4. Validation of the model

Assessing the performance of the groundwater potentiality model (i.e. validation) is considered to be a crucial stage in groundwater management and model selection (Lee et al., 2012a). To examine the reliability and performance of the model, a cross-validation approach and subsequently the receiver operating characteristic (ROC) curve method were used in this study. In the ROC curve method, the sensitivity of the model is plotted against 1-specificity (Tehrany et al., 2013). The area under the ROC curve (AUC) can be used to assess the diagnostic performance of a metric (Chung and Fabbri, 2003). An AUC value of 0 indicates a non-informative model and when AUC equals 1 it indicates perfect model. So, AUC is a very widely used measure of performance due to its understandable, comprehensive and visually attractive way of accuracy assessment (Tehrany et al., 2013). The training groundwater wells (i.e. 70% of inventory groundwater well locations) were used to generate the groundwater potentiality model, but could not be used to evaluate the prediction capability of the DS model. Hence, the model was validated by comparing the acquired groundwater potentiality map with all groundwater wells having with different potentiality including low yield ($<$40 m^3/h) and 30% of groundwater wells with high yield ($>$40 m^3/h) which were not used for training the model. Based on Yesilnacar (2005), the quantitative–qualitative relationship between the AUC value and prediction efficiency can be divided in five classes: 0.5–0.6 (poor), 0.6–0.7 (average), 0.7–0.8 (good), 0.8–0.9 (very good), and 0.9–1 (excellent).

3.5. Groundwater sampling and chemical analysis

Groundwater is an important source of drinking water in the study area and this valuable source is affected by nitrate contamination. Selection of groundwater wells to assess the nitrate concentration was based on the data availability. However, a comprehensive sampling campaign was carried out in the study area during August 2015, which coincided with periods of low water table in the aquifer. In Dezful-Andimeshk region, Khozestan, there are seventy-five municipal wells which are operated by Water Resources Department of Khozestan province. In this research, these seventy-five sampling wells were considered to analyze aquifer nitrate levels (Fig. 5). To provide a representative sample of groundwater, samples from wells were taken at the inlet point of the water treatment works. Samples were collected 30 minutes after the

Please cite this article as: Rahmati, O., Melesse, A.M., Application of Dempster–Shafer theory, spatial analysis and remote sensing for groundwater potentiality and nitrate pollution an..., Sci Total Environ (2016), http://dx.doi.org/10.1016/j.scitotenv.2016.06.176

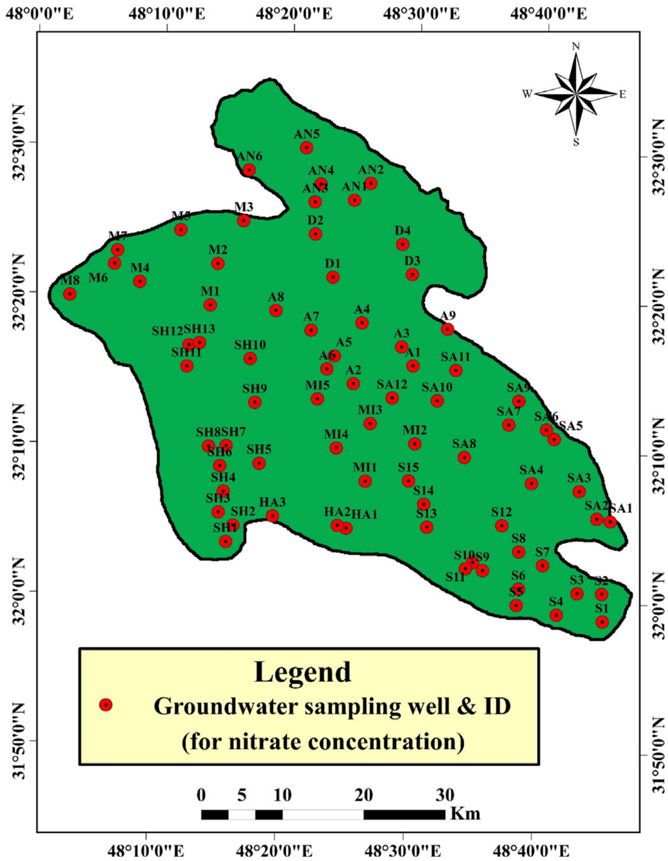

Fig. 5. Geographical position of the groundwater sampling wells (IDs are locational name of sampling wells including AN: Andimeshk, D: Dezful, M: Madani, A: Ayatolh-Montazeri, SH: Shush, MI: Minarood, SA: Saleh-shahr, S: Sardaran, HA: Hafftapeh).

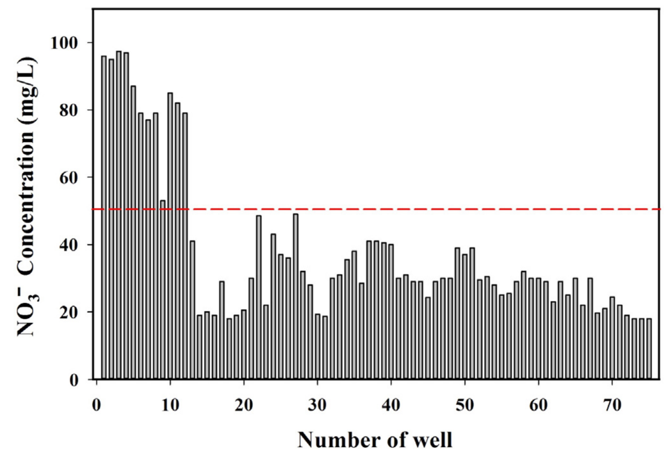

Fig. 6. Nitrate concentrations (mg/L) of sampled wells and the World Health Organization's threshold indicating maximum allowable nitrate concentration for drinking water (red horizontal line).

pump began to run (Fabro et al., 2015). These samples were then filtered in the field through 0.45-μm membrane filters and collected in 60-mL bottles for chemical analysis. Furthermore, all the selected wells were geographically recorded using a GPS.

Groundwater samples were transported to the laboratory with ice bag and examined immediately. In the laboratory, a spectrophotometric analytical method has been developed for the determination of nitrate concentration of groundwater samples. The analysis method can be summarized as follows: (i) preparation of stock nitrate solution; (ii) preparation of standard nitrate solution; (iii) preparation and analysis of standard calibration curve; (iv) spectrophotometric measurements (by Spectrophotometer Uv-vis, Shimadzu, Japan); and (v) determination of nitrate concentration based on standard calibration curve. All the analytical methods were carried out according to the methodologies outlined in the Standard Methods for the Examination of Water and Wastewater (APHA, 2005).

3.6. Assessment of groundwater nitrate pollution

Intense agricultural activities pose a high risk for nitrate leaching into drinking water supplies (McKeon et al., 2005; Re et al., 2014; Kurunc et al., 2016). In our study, after collection and chemical analysis of water samples, the descriptive statistics of groundwater nitrate concentration were generated (Table 2). Nitrate concentrations of sampling wells were compared to the World Health Organization (WHO) maximum specified threshold (50 mg/L) (WHO, 2011) as a reference for drinking water quality guidance (Fig. 6). Referring to Fig. 6, nitrate concentrations of 12 wells (12.9%) out of total number of 75 were higher than the maximum threshold allowable for human consumption. The water quality of 12 wells was of a concern, thus not suitable for human consumption. Therefore, pollution monitoring and water quality assessment in this region need to be conducted accordingly. In this study, the ordinary Kriging (OK) interpolation technique was used for the preparation of groundwater nitrate concentration map since it provided minimal prediction error.

3.7. Construction of groundwater potentiality and quality map

Two steps should be performed to achieve the best groundwater potentiality and quality prediction map. First, the groundwater potentiality map should be reclassified into two classes: (1) poor potential (i.e. merge of low and medium classes) and (2) good potential (i.e. merge of high and very high classes). As shown in Table 3, in the poor potential areas, value of 0 was assigned, while in the good potential areas the value of 1 was given. Second, groundwater nitrates concentration maps were divided in to three classes: <25 mg/L (i.e. concentrations below the guide level), 25–50 mg/L (i.e. between the guide level and the maximum admissible concentration), and >50 mg/L (i.e. concentrations above the maximum admissible concentration) (EU Water Framework Directives 2000/60/EC and 2006/118/EC). In the groundwater nitrates concentration layer, three values 1, −1, and 0 were assigned to <25 mg/L, 25–50 mg/L, and >50 mg/L classes, respectively. The groundwater potentiality and the nitrates concentration raster maps were combined in a GIS environment using Boolean operator function to exclude the final map of groundwater potentiality and quality.

Table 2
Descriptive statistics of groundwater nitrate concentration measured during the year 2013.

Number of samples	Average (mg/L)	Standard deviation	Minimum (mg/L)	Maximum (mg/L)	Median (mg/L)	Skewness	Kurtosis	CV[a] (%)
75	37.70	22.11	7.5	99.75	30	1.60	1.54	58.66

[a] CV: Coefficient of variation.

Table 3
Classifications and values used for the recognition of the areas for groundwater potentiality and quality.

	Class	Description	Value used
Groundwater potentiality	Low and medium	Poor potential	0
	High and very high	Good potential	1
Nitrate concentrations (mg/L)	0–25	Good quality	1
	25–50	Moderate quality (admissible)	−1
	>50	Bad quality (water polluted)	0
Suitability for drinking water	Non acceptable	Poor potential and/or bad quality	0
	Moderate acceptable	Good potential and moderate quality	−1
	Acceptable	Good potential and quality	1

4. Results and discussion

4.1. Application Dempster–Shafer theory in groundwater potentiality mapping

Each of the classes of the nine conditioning factors such as lithology, land use, soil type, altitude, slope percent, distance from river, river density, TWI, and lineament density, were further divided using Eqs. (10), (11), (14) and (15), and into four mass functions that represent the degrees of belief, disbelief, uncertainty and plausibility. Fig. 7 shows integrated maps of DS model. The spatial distribution of these belief functions components can be interpreted in terms of physiography. According to the physiography and distribution of hydrography system, higher degrees of belief (B) and plausibility (P) are correlated with flat areas and near to rivers, while lower degrees are correlated with steep slope areas.

Fig. 8 illustrates the normalized weight values for each classified evidential layer. A comparatively high weight value implies a higher probability of groundwater occurrence, while a low weight value shows a lower probability of groundwater occurrence (Nampak et al., 2014). In

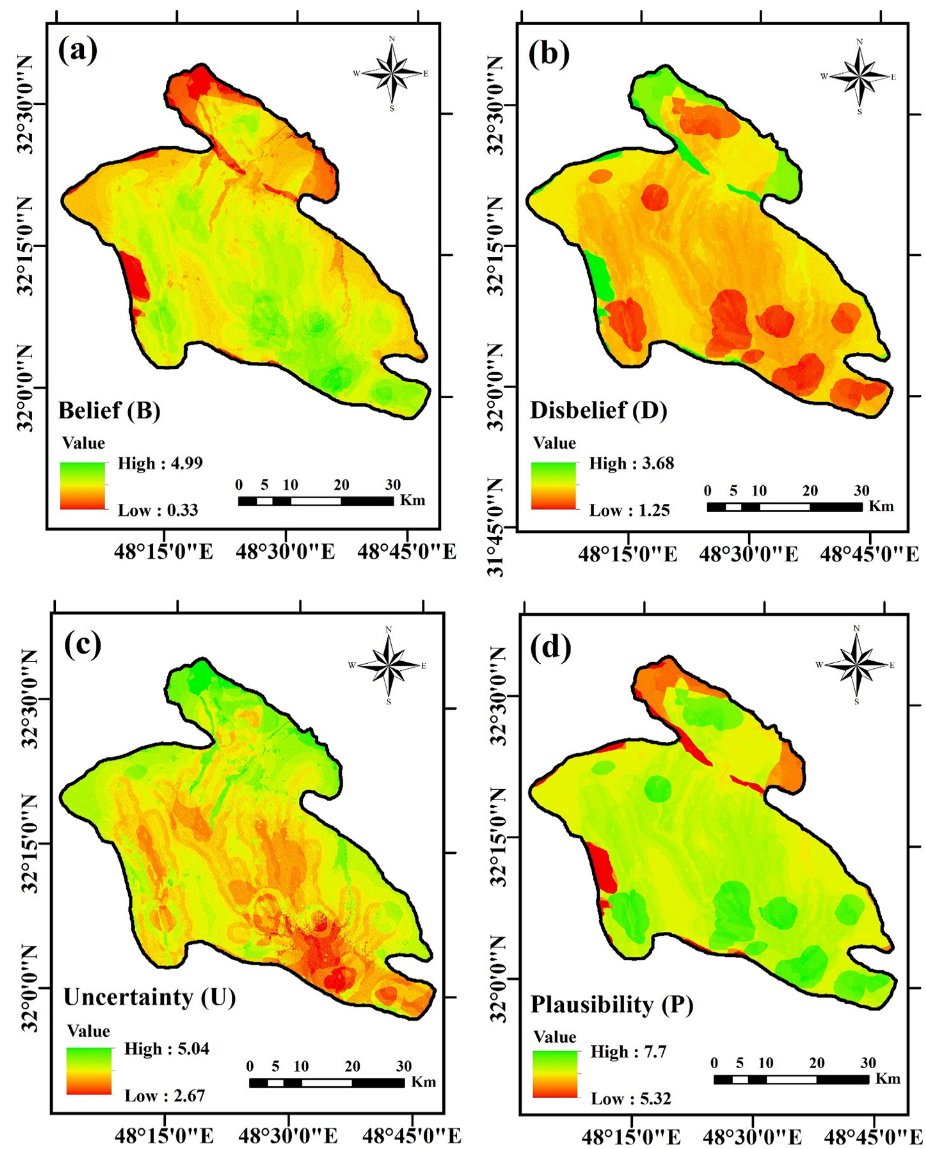

Fig. 7. Integrated results of DS model; (a) belief, (b) disbelief, (c) uncertainty, and (d) plausibility.

the case of lithology, there were two classes according to lithology map of the study area. The weight value, with respect to groundwater occurrence, was higher for the Qft_2 class but there was no relationship between the groundwater well locations and Plbk class (Fig. 8a). In the case of land use, the weight value was higher for irrigated agriculture (0.57), and wetland (0.43) classes followed by riparian zone category (0.28) (Fig. 8b). Irrigation water, which mainly consisted of riverine water, infiltrates back to the saturated aquifer and recharges the aquifer of study area during irrigations (Zeng and Cai, 2014). Therefore, the highest weight value was allocated to the irrigated agriculture among all of the landuse types. In this analysis, very weak relationships were found between groundwater potentiality and dry farming and badland categories.

In the soil type map, high weight value for Inceptisols indicates that this category has a positive spatial association with groundwater occurrence (Fig. 8c). However, very weak relationships were detected between the other soil type categories (i.e. Entisols and badland soil) and the groundwater well locations.

The normalized weight value for altitude and slope percent indicated inverse relationships between such topographic factors and groundwater occurrences. The analysis of normalized weight value for the relationship between groundwater occurrence and altitude indicates that altitude class <50 m has the highest weight value (0.57) followed by 50–100 m class (0.22) (Fig. 8d). Also, assessment of slope percent showed that the class of 0–3 has the highest weight value (0.53) followed by 3–6 class (0.49) (Fig. 8e). The study by Adiat et al. (2012) confirmed that the gentle slope areas promote infiltration and groundwater recharge; hence, these areas have greater probability of groundwater potential.

Distance from river also indicated inverse relationship with groundwater occurrences according to the weight values (Fig. 8f). This finding agrees with Villeneuve et al. (2015) in that, when the distance from river increases, the probability of groundwater occurrence decreases. In the case of river density map, there is a positive correlation between river density and groundwater occurrence which points out a higher groundwater potential over an increasing value of river density (Fig. 8g). The drainage density result matches with the findings of Nampak et al. (2014) that there is a positive relationship between the denser drainage and the greater probability of groundwater potential. These findings also agree with Oikonomidis et al. (2015), which indicated that there is the direct relationship between drainage density and the potentiality of groundwater existence.

This study found that there is a positive correlation between TWI and groundwater productivity (Fig. 8h). Therefore, this result indicated that groundwater potentiality increased with the increase of the TWI value. This result confirms the results of Nampak et al. (2014); Mogaji et al. (2014), and Davoodi Moghaddam et al. (2015) as direct link between the TWI value and groundwater occurrence.

The analysis of DS results for the relationship between groundwater occurrence and lineament density indicates that lineament density class 0.25–0.38 km/km^2 has the highest normalized weight value (0.63) followed by >0.38 km/km^2 class (0.54) (Fig. 8i). These findings agree

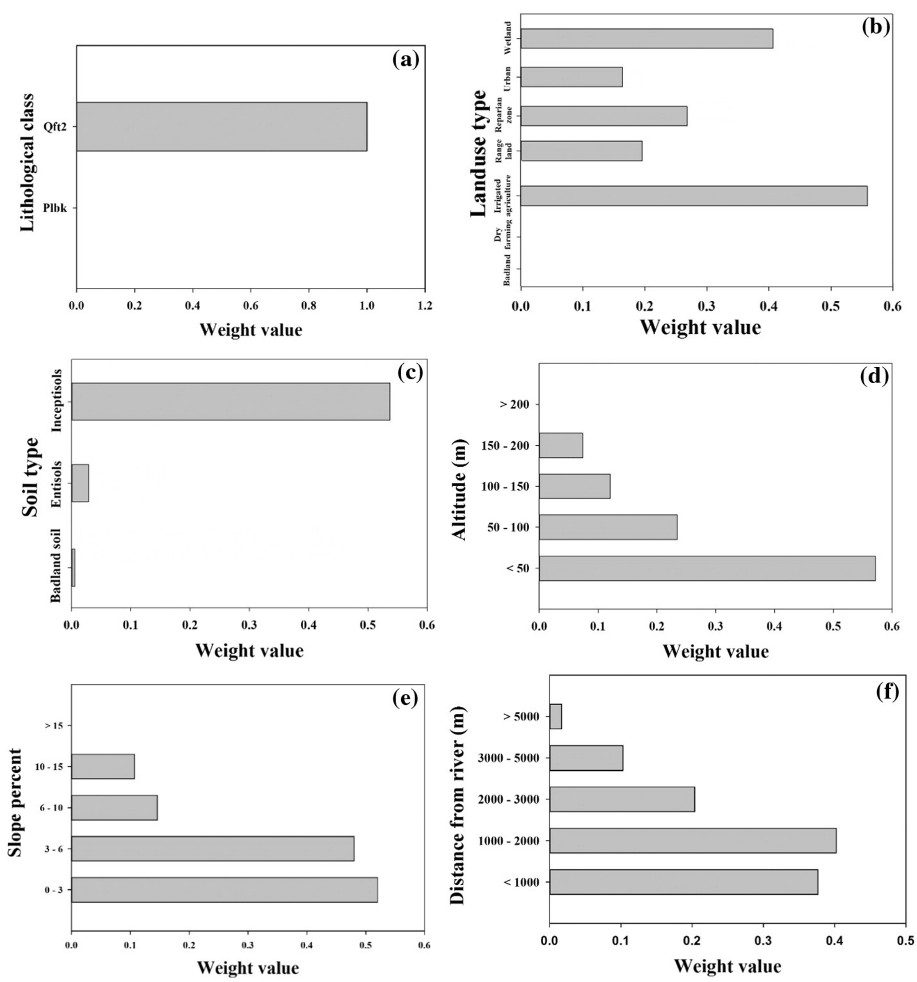

Fig. 8. Weight value of each conditioning factor: (a) lithology, (b) land use, (c) soil type, (d) altitude, (e) slope percent, (f) distance from river, (g) river density, (h) TWI, and (i) lineament density.

Please cite this article as: Rahmati, O., Melesse, A.M., Application of Dempster–Shafer theory, spatial analysis and remote sensing for groundwater potentiality and nitrate pollution an..., Sci Total Environ (2016), http://dx.doi.org/10.1016/j.scitotenv.2016.06.176

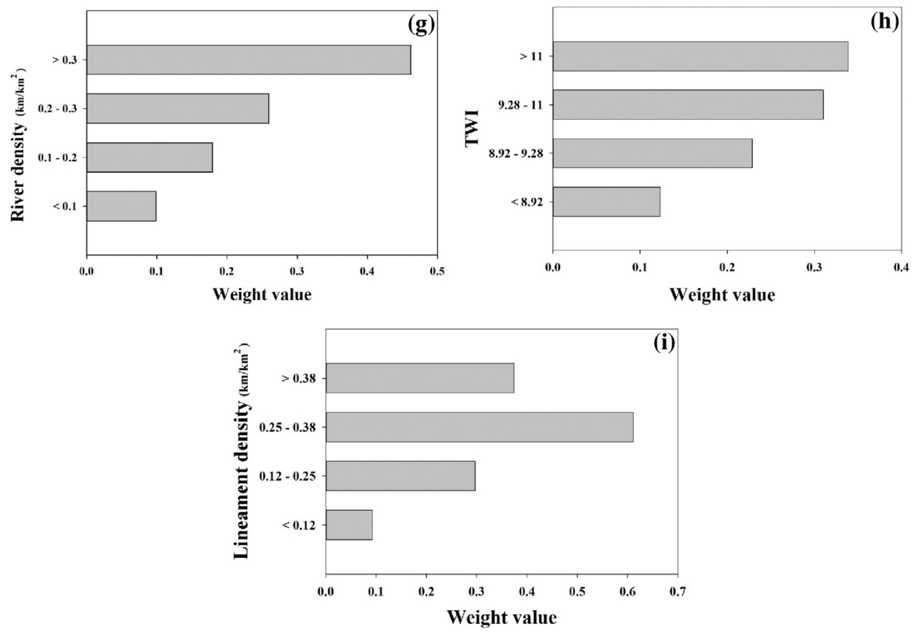

Fig. 8 (*continued*).

with other studies (Sree Devi et al., 2001; Mogaji et al., 2014; Rahmati et al., 2014).

Based on the consideration of weight value obtained from DS model for all conditioning factors, groundwater potentiality map was produced. There are various classification schemes available such as manual, equal intervals, quantile, geometrical intervals, natural breaks (Jenks), and standard deviations (Oh et al., 2011; Lee et al., 2012a,b; Park et al., 2014). In this study, the quantile classification method applied by Nampak et al. (2014) and Razandi et al. (2015) was used to classify the groundwater potentiality map into four classes: low, medium, high, and very high (Fig. 9). The 'high' and 'very high' groundwater potential classes mainly cover central parts of areas around the river systems.

The main advantage of the DS theory of evidence approach is that, unlike other data-driven models, DS model supports a series of mass functions including belief (B), disbelief (D), uncertainty (U) and plausibility (P). Thus, the results can adequately represent quantitative relationships between groundwater occurrences and several geo-environmental layers by using modeling the degree of uncertainty (Mogaji et al., 2014; Park et al., 2014). For example, the uncertainty

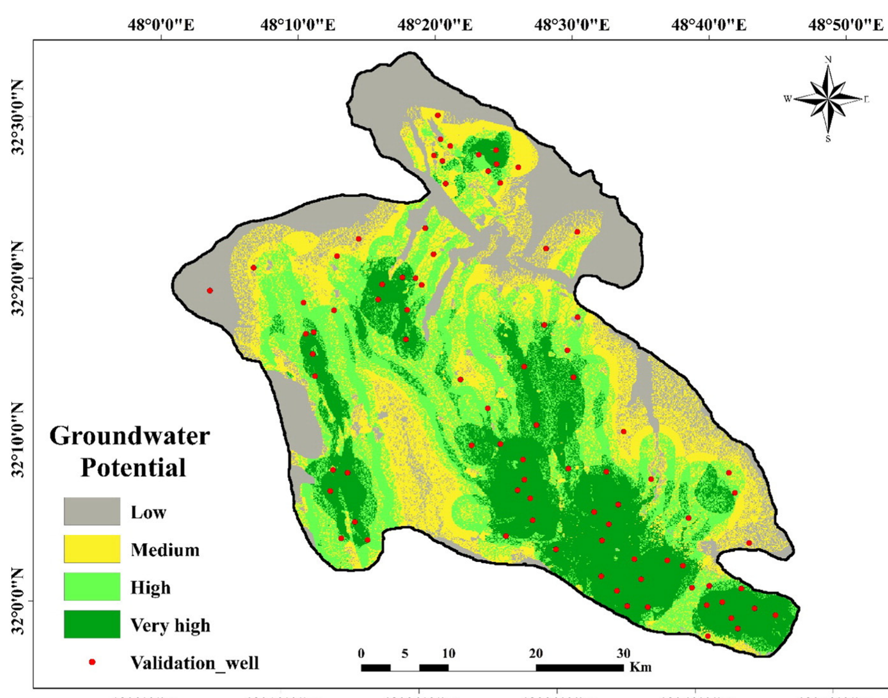

Fig. 9. Distribution of the groundwater potentiality based on DS model.

Please cite this article as: Rahmati, O., Melesse, A.M., Application of Dempster–Shafer theory, spatial analysis and remote sensing for groundwater potentiality and nitrate pollution an..., Sci Total Environ (2016), http://dx.doi.org/10.1016/j.scitotenv.2016.06.176

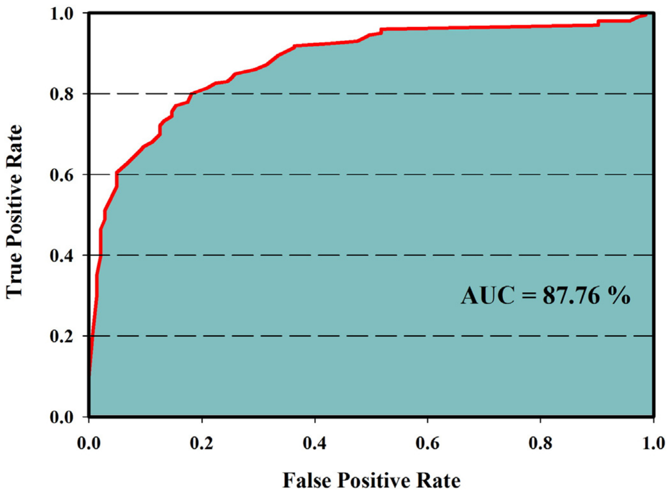

Fig. 10. ROC curve for the groundwater potential maps produced by DS model.

map indicated the presence of insufficient groundwater conditioning layers or a lack of information for groundwater potentiality assessment (Neshat and Pradhan, 2015).

4.2. Validation of groundwater potential map

The GPM should effectively predict distribution of the groundwater potentiality. So, the result of the groundwater potentiality analysis was validated using validation dataset (86 groundwater wells) that were not used for the modeling. The ability of DS model in groundwater potentiality mapping was examined through the use of the area under the curve (AUC) method. For this, ROC curve was constructed for quantitative prediction accuracy, and the AUC was calculated. Fig. 10 illustrates the ROC curve of DS model. The validation of results indicated that the DS model has fairly good prediction accuracy of 87.76% (i.e. AUC = 0.877) which is reasonable for regional groundwater potential mapping. The performance/capability of the DS model is in agreement with the result obtained by other studies applied in groundwater potentiality mapping (Nampak et al., 2014; Mogaji et al., 2014).

Table 4
Prediction error obtained from geostatistical analysis (OK interpolation technique).

Prediction errors	Value
Mean	0.24
Root-mean-square (RMSE)	4.20
Average standard error	3.44
Mean standardized	0.05
Root-mean-square standardized	1.39

4.3. Construction of the groundwater nitrate concentration map

The first groundwater pollution caused by intense agriculture and farming activities, and excess application of nitrogenous fertilizers in the region was identified as nitrate contamination. Nitrate concentration enters the soil, leads to nitrate leaching and percolation into the aquifer to groundwater system, subsequently causing an increase in groundwater nitrate concentrations. To investigate the spatial extent of nitrate contamination, the spatial distribution of nitrate concentration map was extracted through the ordinary Kriging (OK) interpolation technique (see Section 3.6) based on 75 groundwater samples using GIS (Fig. 11a).

The geostatistical analysis was carried out to obtain an estimation of accuracy of the nitrate concentration mapping. The results of geostatistical analysis are shown in Table 4. Mean prediction error (ME) for nitrate concentration map was close to zero, implying an unbiased prediction. Furthermore, the root-mean-square standardized value tends to 1 (1.39), demonstrating accuracy and precision of prepared nitrate concentration map. In addition, a small Root-Mean-Square-Error (RMSE) value indicates similarity between predicted and measured values.

4.4. Construction of groundwater potentiality and quality map

After classification of both groundwater potentiality and groundwater nitrate concentration maps, according to combination strategy presented in Table 3, the final map of groundwater potentiality and quality was produced (Fig. 12). This reveals three distinct zones representing ‘acceptable’, ‘moderately acceptable’, and ‘non-acceptable’ suitability for drinking water in the area. The suitability for drinking water in the eastern portion and parts of northwest, north and center

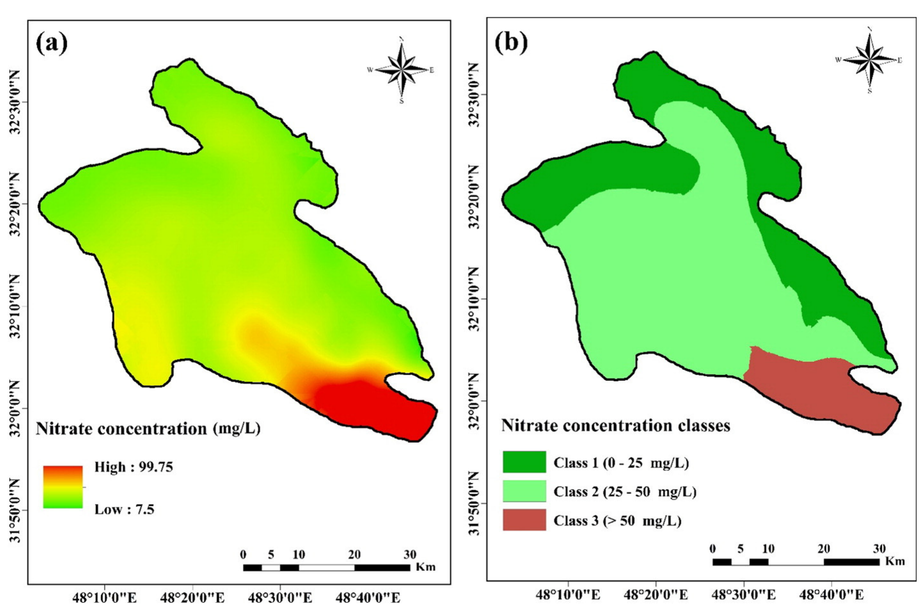

Fig. 11. Evaluation of the nitrate pollution in groundwater over the study area: (a) spatial distribution of nitrate concentration; (b) classification of the nitrate concentration.

Please cite this article as: Rahmati, O., Melesse, A.M., Application of Dempster–Shafer theory, spatial analysis and remote sensing for groundwater potentiality and nitrate pollution an..., Sci Total Environ (2016), http://dx.doi.org/10.1016/j.scitotenv.2016.06.176

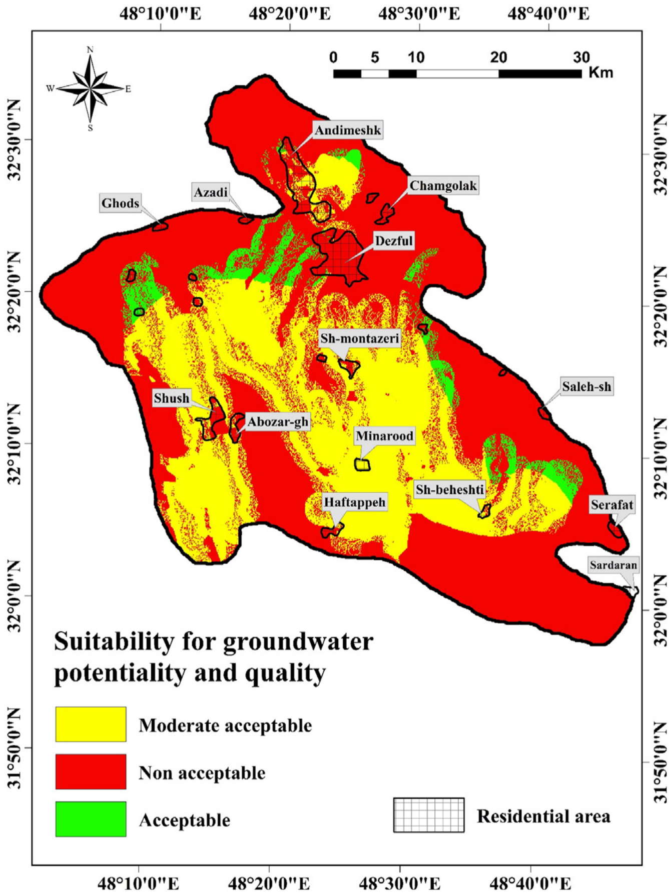

Fig. 12. Suitability map for groundwater potentiality and quality showing main residential areas in the Dezful-Andimeshk region, Khozestan, Iran.

of the study area is 'acceptable', covering an area of 100.3 km^2, which is 4.1% of the total area. In addition, the central portion and some small patches in the west and north portions of the study area fall under 'moderately acceptable' groundwater suitability for drinking water purpose, encompassing an area of 886.6 km^2, which is about 36% of the total study area. The 'non-acceptable' class covers the largest part of the study area with 60% (i.e. 1,477.9 km^2) and is located in the south, eastern, north and north-western parts and some small patches in the center of the study area. However, in the 'moderately acceptable' class, the monitoring and management of the groundwater hydrochemistry should be more regular in the groundwater wells which are used for domestic use and human consumption.

5. Conclusions

In groundwater management and/or monitoring of arid and semi-arid regions, water quality and quantity are two vital components of comprehensive management of groundwater resources, that their integration and conjunction assessment are scientifically needed. The study was intended to evaluate the performance of the DS theory of evidence approach for predictive modeling of groundwater potentiality and combination of its results with the nitrate concentration map to provide high quality reliable drinking water in the Andimeshk-Dezful region, Khozestan province, Iran. Hence, this new methodological framework, not only illustrates the areas of groundwater existence potentiality, but also shows areas affected by non-polluted groundwater. In addition, the probability and uncertainty for a spatial distribution of groundwater potentiality were considered through DS model. This study showed that the DS model is ideal for groundwater potential modeling and for simulating the sophisticated relationship between geo-environmental factors and groundwater productivity/occurrence, which allows analysis of both stochastic and systemic uncertainty. Furthermore, it can be concluded that DS model can be applied as a cost-effective approach for groundwater potential modeling and to fill management gaps in the current groundwater resources planning.

Moreover, groundwater potentiality and quality map is very useful for the decision-makers and can be used to (i) identify areas that currently are at "acceptable" category for drinking water supply, (ii) protect water supplies in these good-quality areas which have high groundwater productivity, and (iii) establish pollution monitoring and water quality assessment programs, especially for 'moderate acceptable' areas. However, the applied approach has two main drawbacks: (1) because the weight values are dependent on the number of groundwater wells used on the spatial analysis, the models underestimates or overestimates groundwater potential condition if the groundwater wells are not evenly distributed and/or the area of a factor class is very small, and (2) the geo-environmental factors may have not thoroughly independence condition.

Acknowledgments

We are grateful to the Editor, Prof. Ashantha Goonetilleke, and three anonymous referees for their constructive comments which were valuable to improve our manuscript. We would like to thanks Dr. Hamid Reza Pourghasemi for his assistance in implementation of the DS model. Also, we thank to Water Resources Department of Khozestan province and Iranian Department of Geology Survey (IDGS) for providing necessary data and maps.

References

Adiat, K.A.N., Nawawi, M.N.M., Abdullah, K., 2012. Assessing the accuracy of GIS-based elementary multi criteria decision analysis as a spatial prediction tool—a case of predicting potential zones of sustainable groundwater resources. J. Hydrol. 440, 75–89.

Alavi, M., 1994. Tectonics of the Zagros orogenic belt of Iran; new data and interpretations. Tectonophysics 229, 211–238.

American Public Health Association (APHA), 2005. American Water Works Association and Water Pollution Control Federation. Standard methods for the examination of water and wastewater, 13th ed. Amerircan Public Health Association (APHA), Washington, DC.

Carranza, E.J.M., Woldai, T., Chikambwe, E.M., 2005. Application of data-driven evidential belief functions to prospectivity mapping for aquamarine-bearing pegmatites, Lundazi district, Zambia. Nat. Resour. Res. 14 (1), 47–63.

Chandrakanth, M.G., 2015. Sustainable path of extraction of groundwater in tank and canal command areas. Water Resource Economics. Springer, India, pp. 173–189 http://dx.doi.org/10.1007/978-81-322-2479-2_12.

Chen, J., Xue, L., 2003. Is ground-water in arid inland drainage basins a resource for sustainable development? J. Arid Environ. 55, 389–390.

Chung, C.F., Fabbri, A.G., 2003. Validation of spatial prediction models for landslide hazard mapping. Nat. Hazards 30, 451–472.

Davoodi Moghaddam, D., Rezaei, M., Pourghasemi, H.R., Pourtaghie, Z.S., Pradhan, B., 2015. Groundwater spring potential mapping using bivariate statistical model and GIS in the taleghan watershed Iran. Arab. J. Geosci. 8 (2), 913–929.

Dempster, A.P., 1967. Upper and lower probabilities induced by a multivalued mapping. Ann. Math. Stat. 38, 325–339.

Elewa, H.H., Qaddah, A.A., 2011. Groundwater potentiality mapping in the Sinai Peninsula, Egypt, using remote sensing and GIS-watershed-based modeling. Hydrogeol. J. 19, 613–628.

Elmahdy, S.I., Mohamed, M.M., 2014. Groundwater potential modelling using remote sensing and GIS: a case study of the Al Dhaid area, United Arab Emirates. Geocarto Int. http://dx.doi.org/10.1080/10106049.2013.784366.

Elmahdy, S.I., Mohamed, M.M., 2015. Groundwater of Abu Dhabi Emirate: a regional assessment by means of remote sensing and geographic information system. Arab. J. Geosci. http://dx.doi.org/10.1007/s12517-015-1932-2.

Fabro, A.Y.R., Ávila, J.G.P., Alberich, M.V.E., Sansores, S.A.C., Camargo-Valero, M.A., 2015. Spatial distribution of nitrate health risk associated with groundwater use as drinking water in Merida, Mexico. Appl. Geogr. 65, 49–57.

Falah, F., Ghorbani Nejad, S., Rahmati, O., Daneshfar, M., Zeinivand, H., 2016. Applicability of generalized additive model in groundwater potential modelling and comparison its performance by bivariate statistical methods. Geocarto Int. http://dx.doi.org/10.1080/10106049.2016.1188166.

Ghorbani Nejad, S., Falah, F., Daneshfar, M., Haghizadeh, A., Rahmati, O., 2016. Delineation of groundwater potential zones using remote sensing and GIS-based data-driven models. Geocarto Int. http://dx.doi.org/10.1080/10106049.2015.1132481.

Heyvaert, V.M.A., Baeteman, C., 2007. Holocene sedimentary evolution and palaeocoastlines of the Lower Khuzestan plain (southwest Iran). Mar. Geol. 242, 83–108.

Jalali, M., 2011. Nitrate pollution of groundwater in Toyserkan, Western Iran. Environ. Earth Sci. 62, 907–913.

Jha, M.K., Chowdary, V.M., Chowdhury, A., 2010. Groundwater assessment in Salboni Block, West Bengal (India) using remote sensing, geographical information system and multi-criteria decision analysis techniques. Hydrogeol. J. 18, 1713–1728.

Kim, H., Swain, P.H., 1989. Multisource data analysis in remote sensing and geographic information systems based on Shafer's theory of evidence. Proceedings of 1989 International Geoscience and Remote Sensing Symposium, pp. 829–832.

Kurunc, A., Ersahin, S., Sonmez, N.K., Kaman, H., Uz, I., Uz, B.Y., Aslan, G.E., 2016. Seasonal changes of spatial variation of some groundwater quality variables in a large irrigated coastal Mediterranean region of Turkey. Sci. Total Environ. 554–555, 53–63.

Lee, S., Kim, Y.S., Oh, H.J., 2012a. Application of a weights-of-evidence method and GIS to regional groundwater productivity potential mapping. J. Environ. Manag. 96, 91–105.

Lee, S., Song, K.Y., Kim, Y., Park, I., 2012b. Regional groundwater productivity potential mapping using a geographic information system (GIS) based artificial neural network model. Hydrogeol. J. 20, 1511–1527.

Lillesand, M.T., Kiefer, W.R., Chipman, J., 2008. Remote Sensing and Image Interpretation. sixth ed. Wiley, New York (768 pp.).

Manap, M.A., Sulaiman, W.N.A., Ramli, M.F., Pradhan, B., Surip, N., 2013. A knowledge-driven GIS modeling technique for groundwater potential mapping at the Upper Langat Basin, Malaysia. Arab. J. Geosci. 6, 1621–1637.

Masoud, A.A., Koike, K., Mashaly, H.A., Gergis, F., 2016. Spatio-temporal trends and change factors of groundwater quality in an arid area with peat rich aquifers: emergence of water environmental problems in Tanta District, Egypt. J. Arid Environ. 124, 360–376.

McKeon, C.A., Jordan, F.L., Glenn, E.P., Waugh, W.J., Nelson, S.G., 2005. Rapid nitrate loss from a contaminated desert soil. J. Arid Environ. 61, 119–136.

McLay, C.D.A., Dragten, R., Sparling, G., Selvarajah, N., 2001. Predicting groundwater nitrate concentrations in a region of mixed agricultural land use: a comparison of three approaches. Environ. Pollut. 115, 191–204.

Mills, A.C., Shata, A., 2009. Ground-water assessment of Sinai, Egypt. Groundwater 27 (6), 793–801.

Mogaji, K.A., Lim, H.S., Abdullah, K., 2014. Regional prediction of groundwater potential mapping in a multifaceted geology terrain using GIS-based Dempster–Shafer model. Arab. J. Geosci. http://dx.doi.org/10.1007/s12517-014-1391-1.

Moore, I.D., Grayson, R.B., Ladson, A.R., 1991. Digital terrain modeling: a review of hydrological, geomorphological and biological applications. Hydrol. Process. 5, 3–30.

Nampak, H., Pradhan, B., Manap, M.A., 2014. Application of GIS based data driven evidential belief function model to predict groundwater potential zonation. J. Hydrol. 513, 283–300.

Neshat, A., Pradhan, B., 2015. Risk assessment of groundwater pollution with a new methodological framework: application of Dempster–Shafer theory and GIS. Nat. Hazards http://dx.doi.org/10.1007/s11069-015-1788-5.

Oh, H.J., Kim, Y.S., Choi, J.K., Park, E., Lee, S., 2011. GIS mapping of regional probabilistic groundwater potential in the area of Pohang City, Korea. J. Hydrol. 399, 158–172.

Oikonomidis, D., Dimogianni, S., Kazakis, N., Voudouris, K., 2015. A GIS/Remote Sensing-based methodology for groundwater potentiality assessment in Tirnavos area, Greece. J. Hydrol. 525, 197–208.

Ozdemir, A., 2011. GIS-based groundwater spring potential mapping in the Sultan Mountains (Konya, Turkey) using frequency ratio, weights of evidence and logistic regression methods and their comparison. J. Hydrol. 411 (3–4), 290–308.

Park, L., Kim, Y., Lee, S., 2014. Groundwater productivity potential mapping using evidential belief function. Groundwater 52, 201–207.

Park, N.W., 2010. Application of Dempster–Shafer theory of evidence to GIS-based landslide susceptibility analysis. Environ. Earth Sci. 62 (2), 367–376.

Pathak, D.R., Hiratsuka, A., 2011. An integrated GIS based fuzzy pattern recognition model to compute groundwater vulnerability index for decision making. J. Hydro Environ. Res. 5, 63–77.

Pourghasemi, H.R., Beheshtirad, M., 2014. Assessment of a data-driven evidential belief function model and GIS for groundwater potential mapping in the Koohrang Watershed, Iran. Geocarto Int. http://dx.doi.org/10.1080/10106049.2014.966161.

Pourtaghi, Z.S., Pourghasemi, H.R., 2014. GIS-based groundwater spring potential assessment and mapping in the Birjand Township, southern Khorasan Province Iran. Hydrogeol. J. 22 (3), 643–662.

Pradhan, B., 2009. Groundwater potential zonation for basaltic watersheds using satellite remote sensing data and GIS techniques. Open Geosci. 1 (1), 120–129.

Rahmati, O., Nazari Samani, A., Mahdavi, M., Pourghasemi, H.R., Zeinivand, H., 2014. Groundwater potential mapping at Kurdistan region of Iran using analytic hierarchy process and GIS. Arab. J. Geosci. doi http://dx.doi.org/10.1007/s12517-014-1668-4.

Rahmati, O., Nazari Samani, A., Mahmoodi, N., Mahdavi, M., 2015. Assessment of the contribution of N-fertilizers to nitrate pollution of groundwater in western Iran (Case Study: Ghorveh–Dehgelan Aquifer). Water Qual Expo Health 7 (2), 143–151.

Rahmati, O., Pourghasemi, H.R., Melesse, A.M., 2016. Application of GIS-based data driven random forest and maximum entropy models for groundwater potential mapping: a case study at Mehran Region, Iran. Catena 137, 360–372.

Razandi, Y., Pourghasemi, H.R., Samani Neisani, N., Rahmati, O., 2015. Application of analytical hierarchy process, frequency ratio, and certainty factor models for groundwater potential mapping using GIS. Earth Sci. Inform. http://dx.doi.org/10.1007/s12145-015-0220-8.

Re, V., Sacchi, E., Mas-Pla, J., Menció, A., Amran, N.E., 2014. Identifying the effects of human pressure on groundwater quality to support water management strategies in coastal regions: a multi-tracer and statistical approach (Bou-Areg region, Morocco). Sci. Total Environ. 500–501, 211–223.

Rodhe, A., Seibert, J., 1999. Wetland occurrence in relation to topography: a test of topographic indices as moisture indicators. Agric. For. Meteorol. 98–99, 325–340.

Sajil, K.P.J., Jegathambal, P., James, E.J., 2014. Chemometric evaluation of nitrate contamination in the groundwater of a hard rock area in Dharapuram, South India. Appl Water Sci 4, 397–405.

Saraf, A.K., Choudhury, P.R., 1998. Integrated remote sensing and GIS for ground water exploration and identification of artificial recharges sites. Int. J. Remote Sens. 19 (10), 1825–1841.

Shafer, G.A., 1976. Mathematical Theory of Evidence. Princeton University Press, Princeton, pp. 1–24.

Shekhar, S., Pandey, A.C., 2014. Delineation of groundwater potential zone in hard rock terrain of India using remote sensing, geographical information system (GIS) and analytic hierarchy process (AHP) techniques. Geocarto Int. http://dx.doi.org/10.1080/10106049.2014.894584.

Sree Devi, P.D.S., Srinivasulu, S., Raju, K.K., 2001. Hydrogeomorphological and groundwater prospects of the Pageru river basin by using remote sensing data. Environ. Geol. 40, 1088–1094.

Sternberg, T., Paillou, P., 2015. Mapping potential shallow groundwater in the Gobi Desert using remote sensing: Lake Ulaan Nuur. J. Arid Environ. 118, 21–27.

Suthar, S., Bishnoi, P., Singh, S., Mutiyar, P.K., Nema, A.K., Patil, N.S., 2009. Nitrate contamination in groundwater of some rural areas of Rajasthan, India. J. Hazard. Mater. 171 (1–3), 189–199.

Tahmassebipoor, N., Rahmati, O., Noormohamadi, F., Lee, S., 2015. Spatial analysis of groundwater potential using weights-of-evidence and evidential belief function models and remote sensing. Arab. J. Geosci. doi http://dx.doi.org/10.1007/s12517-015-2166-z.

Tam, V.T., De Smedt, F., Batelaan, O., Dassargues, A., 2004. Study on the relationship between lineaments and borehole specific capacity in a fractured and karstified limestone area in Vietnam. Hydrogeol. J. 12, 662–673.

Tehrany, M.S., Pradhan, B., Jebur, M.N., 2013. Spatial prediction of flood susceptible areas using rule based decision tree (DT) and a novel ensemble bivariate and multivariate statistical models in GIS. J. Hydrol. 504, 69–79.

Todd, D.K., Mays, L.W., 1980. Groundwater Hydrology. second ed. Wiley Canada, New York.

Travaglia, C., Dianelli, N., 2003. Groundwater Search by Remote Sensing: A Methodological Approach. FAO. Environment and Natural Resources Service Sustainable Development Department, ROME, p. 34.

USGS, 2015. Landsat 7 ETM+ Images. http://earthexplorer.usgs.gov (Accessed on January 14, 2015).

Villeneuve, S., Cook, P.G., Shanafield, M., Wood, C., White, N., 2015. Groundwater recharge via infiltration through an ephemeral riverbed, central Australia. J. Arid Environ. 117, 47–58.

Walley, P., 1987. Belief function representations of statistical evidence. Ann. Stat. 15, 1439–1465.

[WHO] World Health Organization, 2011. Guidelines for Drinking-water Quality. fourth ed. http://www.who.int/water_sanitation_health/publications/2011/dwq_guidelines/en/.

Xue, D., Pang, F., Meng, F., Wang, Z., Wu, W., 2015. Decision-tree-model identification of nitrate pollution activities in groundwater: a combination of a dual isotope approach and chemical ions. J. Contam. Hydrol. 180, 25–33.

Yesilnacar, E.K., 2005. The Application of Computational Intelligence to Landslide Susceptibility Mapping in Turkey (Ph.D Thesis) Department of Geomatics the University of Melbourne, p. 423.

Zeng, R., Cai, X., 2014. Analyzing streamflow changes: irrigation-enhanced interaction between aquifer and streamflow in the Republican River basin. Hydrol. Earth Syst. Sci. 18, 493–502.